JOURNAL OF NATURAL PRODUCTS

pubs.acs.org/jnp

Article

Campafungins: Inhibitors of *Candida albicans* and *Cryptococcus neoformans* Hyphal Growth

Bruno Perlatti, Guy Harris, Connie B. Nichols, Dulamini I. Ekanayake, J. Andrew Alspaugh, James B. Gloer, and Gerald F. Bills*

Cite This: https://dx.doi.org/10.1021/acs.jnatprod.0c00641

Read Online

ACCESS | Metrics & More | Article Recommendations | Supporting Information

ABSTRACT: Campafungin A is a polyketide that was recognized in the *Candida albicans* fitness test due to its antiproliferative and antihyphal activity. Its mode of action was hypothesized to involve inhibition of a cAMP-dependent PKA pathway. The originally proposed structure appeared to require a polyketide assembled in a somewhat unusual fashion. However, structural characterization data were never formally published. This background stimulated a reinvestigation in which campafungin A and three closely related minor constituents were purified from fermentations of a strain of the ascomycete fungus *Plenodomus enteroleucus*. Labeling studies, along with extensive NMR analysis, enabled assignment of a revised structure consistent with conventional polyketide synthetic machinery. The structure elucidation of campafungin A and new analogues encountered in this study, designated here as campafungins B, C, and D, is presented, along with a proposed biosynthetic route. The antimicrobial spectrum was expanded to methicillin-resistant *Staphylococcus aureus*, *Candida tropicalis*, *Candida glabrata*, *Cryptococcus neoformans*, *Aspergillus fumigatus*, and *Schizosaccharomyces pombe*, with MICs ranging as low as 4−8 μg mL^{-1} in *C. neoformans*. Mode-of-action studies employing libraries of *C. neoformans* mutants indicated that multiple pathways were affected, but mutants in PKA/cAMP pathways were unaffected, indicating that the mode of action was distinct from that observed in *C. albicans*.

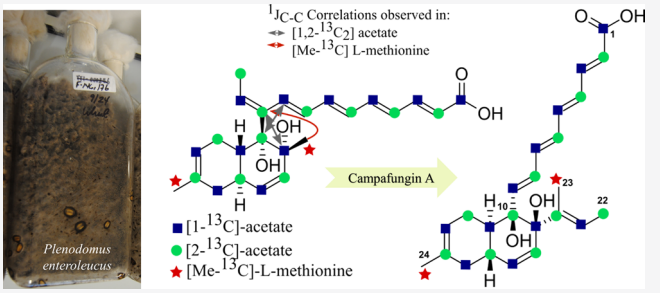

The *Candida albicans* fitness test (CaFT) is a genomics-based approach to discovering novel antifungal agents.[1] The platform consists of 5400 heterozygous *C. albicans* strains in which one allele of a target gene had been deleted, rendering each strain hypersensitive to inhibitors of the target gene. Evaluation of a pure compound or natural product extract against the pool of 5400 strains was able to reveal a pattern from affected hypersensitive strains that could be correlated with the mode of action (MOA) of the anti-*Candida* component. Evaluation of these patterns and those from reference experiments with antifungal agents having known MOAs has proven to be an effective tool for the discovery of novel antifungal natural products and efficient dereplication of natural product extracts.[1−3] Crude fermentation extracts exhibiting a minimal growth inhibition of *C. albicans* in a liquid dilution assay were directly evaluated in the CaFT. Testing of prescreened natural product extracts allowed the development of a straightforward, large-scale natural product screening strategy capable of detecting molecules effective against a broad array of known and novel targets. Application of this strategy with microbial natural products resulted in the discovery of the parnafungins,[4,5] inhibitors of mRNA processing, a previously undescribed antifungal target; natural product and synthetic inhibitors of the glycosylphosphatidylinositol (GPI) anchor pathway;[6] inhibitors of elongation factor 3 (EF3), a fungal selective protein synthesis target;[3] new analogues of inhibitors of more established antifungal targets; and several other new natural products for which the precise MOAs remain unresolved.[7−9]

During screening of *C. albicans*-active natural product extracts at Merck Research Laboratories, a unique and complex CaFT profile was obtained from fermentation extracts of a strain of *Plenodomus enteroleucus* (Ascomycota, Pleosporales) and was prioritized for investigation The responsible metabolite, named campafungin, was assigned a proposed structure and a brief hypothesis for its MOA was offered.[3] Although campafungin exhibited modest potency, the CaFT profile exhibited hypersensitivity to CRY1 (adenylate cyclase) and PRS3 (phosphoribosyl pyrophosphate synthetase) and hyposensitivity to PDE2 (a phosphodiesterase that converts cAMP to AMP) and BCY1 (the protein kinase A/PKA negative regulatory subunit). This pattern of heterozygote sensitivity and resistance was consistent with an effect on the cAMP-dependent PKA pathway and suggested that the active

Received: June 9, 2020

component was affecting cAMP levels.[3] When activated, this pathway induces hyphal growth.[10] Developmental transitions between single-cell yeast and multicellular filaments are essential steps in virulence of diverse fungal pathogens, and the ability of *C. albicans* to cause disease has been strongly linked to the yeast−hyphal conversion.[11,12] For the important human fungal pathogen *C. albicans*, filamentation is thought to be required for immune cell escape via induction of an inflammatory programmed cell death.[13] A recent example of a natural product inhibiting the yeast−hyphal transitions in *C. albicans* is plagicosin F, a sesquiterpenoid from the liverwort *Plagiochila fruticosa*, that was shown to modulate the MAPKA pathway presumably via down-regulation of the cAMP-PKA pathway.[14] Therefore, a small molecule interfering with filamentation would be potentially useful as an agent to attenuate virulence in *C. albicans*.

The original report of campafungin only described the activity against *C. albicans*. Campafungin was characterized as having the formula $C_{24}H_{30}O_4$ and a structure composed of a pentaenoic acid unit linked to a decalin core in an unusual fashion, with the connection occurring along the conjugated chain at C-10 (Figure 1). However, a detailed structural characterization was never published.

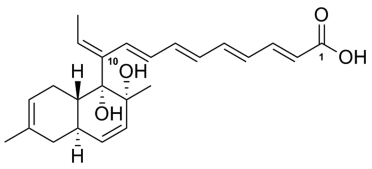

Figure 1. Structure of campafungin originally proposed by Roemer et al. (2011).[3]

We obtained the producing strain in order to understand the biosynthetic origin of the proposed structure of campafungin and to further explore its antifungal spectrum in other human pathogens, e.g., *Cryptococcus neoformans*, as well as its potential mechanisms of antihyphal proliferation. To the best of our knowledge, no other natural structure had been described with a molecular scaffold having a C−C linkage at C-10 as originally proposed. Therefore, we were motivated to explore the biosynthetic origin of the compound by feeding studies with isotopically labeled acetate and methionine.

Herein, we describe the fermentation, bioactivity-guided purification, isotope-labeling studies, structure revision, biosynthetic hypothesis, and biological activity of campafungin, renamed in this article as campafungin A (**1**), and three new minor variants (**2**−**4**). We propose revising the name of the major component to campafungin A to distinguish it from these other co-produced, closely related minor analogues, which we named as campafungins B, C, and D.

RESULTS AND DISCUSSION

Characterization of the Campafungin-Producing Strain. BLAST searches with the LSU and ITS rDNA sequences from strain F-146,176 indicated that it belongs to the genus *Plenodomus* (Pleosporales), and it exhibited high sequence similarity to a complex of species, including *P. enteroleucus*, *P. incompta*, and *P. hendersoniae*.[15] Strain F-146,176 was identified as *P. enteroleucus* based on alignment and maximum likelihood analysis of the combined ITS and LSU with sequences (Figure S1A) from a previous phylogenetic revision of fungi of the Leptosphaeriaceae.[15] Formation of pycnidial conidiomata on agar media was consistent with descriptions of *Plenodomus* species (Figure S1B−E).

Detection of Campafungins from Strain F-146,176. To confirm that strain F-146,176 continued to produce campafungin(s) and to find a medium that would support campafungin production, the strain was grown on five different media. Extracts from Wheat 1 and GS media cultures (see Experimental Section) caused conspicuous inhibitory zones on plates seeded with *C. albicans*, while smaller, but clear zones of inhibition were evident on plates seeded with *C. neoformans*. The extracts from Wheat 1 medium cultures also caused inhibition of *Staphylococcus aureus* (Figure S2). The solid-substrate Wheat 1 medium was selected for large-scale production of campafungins based on the inhibition zone assay results, while the GS medium was used for feeding studies, as liquid media facilitate the homogeneous incorporation of isotope-labeled compounds.

Isolation and Purification of Campafungins. Campafungin A was originally isolated at Merck Research Laboratories from acetone extracts of F-146,176 through bioactivity-guided fractionation.[3] The initial small-scale isolation employed a standardized two-step process consisting of adsorption/gradient elution onto Mitsubishi CHP20Y combined with gradient elution followed by elution-extrusion countercurrent chromatography (EECCC) of the campafungin-rich fraction. The process was guided by antifungal activity against wild-type *C. albicans* as a surrogate for the profile observed using the CaFT. Campafungin A accounted for most of the antifungal activity observed in the crude extracts. Several related minor components were evident, but none appeared more potent than campafungin A. Larger quantities of campafungin A were obtained from EtOAc extracts of F-146,176 liquid fermentation broth using EECCC employing an optimized solvent system of hexane−EtOAc−MeOH−water (5:3:5:3).

For the work described herein, campafungins were obtained as the main fermentation products of *P. enteroleucus* in the tested media. Analysis of the flash chromatography fraction containing campafungins showed one major component and three minor related metabolites, as well as traces of several other compounds (Figure S3). Semipreparative HPLC of the campafungin-rich fraction obtained from flash chromatography afforded campafungin A (**1**) along with three new analogues, **2**−**4**, all of them as light yellow powders.

Structure Elucidation of Campafungins A−D. The molecular formula of campafungin A (**1**) was confirmed as the expected $C_{24}H_{30}O_4$ by HRESIMS analysis. ^{1}H and ^{13}C NMR spectra of freshly isolated **1** were collected in $CDCl_3$ (Figures S4 and S5). ^{1}H NMR data were also acquired in DMSO-d_6 and compared to unpublished spectroscopic data that were originally used to characterize the structure proposed in the original article. Comparison of these data confirmed that the two samples are the same (Figure S6).

Samples of compound **1** obtained from fermentations of *P. enteroleucus* fed with [1-^{13}C]-acetate, [2-^{13}C]-acetate, [1,2-$^{13}C_2$]-acetate, and [Me-^{13}C]-L-methionine showed enrichment of all 24 carbons in the structure, as observed in ^{13}C NMR spectra (Figures S7−S10), with an enrichment of 11 carbons in each of the products obtained using the C_1- and C_2-labeled acetates and two carbons enriched in the product obtained upon feeding with [Me-^{13}C]-L-methionine. The

https://dx.doi.org/10.1021/acs.jnatprod.0c00641
J. Nat. Prod. XXXX, XXX, XXX−XXX

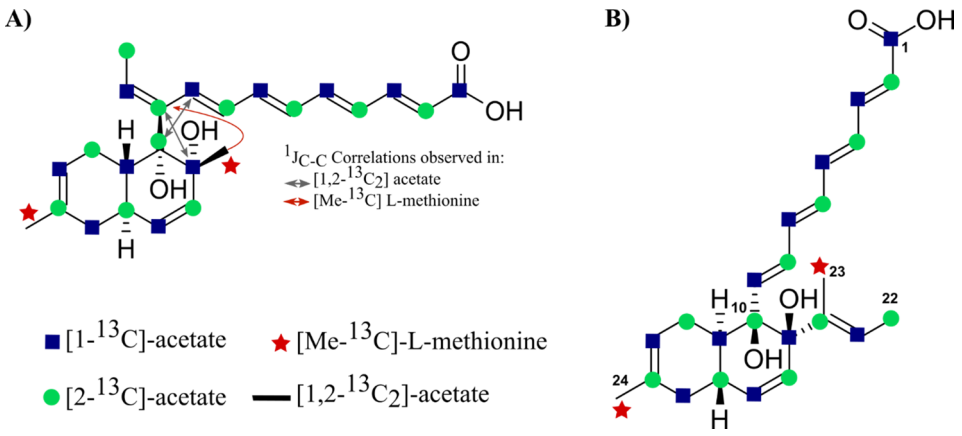

Figure 2. (A) Enrichment pattern observed imposed onto the original structure, highlighting the incorrect assignments revealed by $^{1}J_{C-C}$ coupling observed in the ^{13}C NMR spectrum of the [Me-^{13}C]-L-methionine-labeled product. (B) New structure assigned based on biosynthetic and NMR data obtained in this study.

number of labeled carbon atoms observed in campafungin A for each labeled acetate was indicative of a typical polyketide backbone. When correlated with the original ^{13}C NMR assignments, the collective acetate and methionine labeling results would require an extensive rearrangement relative to typical polyketide biosynthesis (Figure 2)[16] or some other unknown biosynthetic route. This led us to question the original assignment and to undertake independent detailed analysis of the structure by 2D NMR.

A set of 2D NMR data (COSY, HSQC, HMBC, and NOESY) was acquired for campafungin A in $CDCl_3$ (Figures S11−S15). Analysis of the ^{13}C NMR and HSQC data showed 24 carbon signals, including three methyls, two sp^3 methylenes, two sp^3 methines, two oxygen-bearing nonprotonated sp^3 carbons, 14 sp^2 carbons, and a carboxy carbonyl, indicating the presence of seven olefin units and two rings, as was the case for the originally proposed structure. The ^{1}H NMR spectrum showed overlapping signals for three vinylic methyl groups, as well as multiplets corresponding to six sp^3 hydrogens and 12 sp^2 hydrogens, all of which could be assigned to attached carbons on the basis of the HSQC data. HMBC correlations from olefinic hydrogens H-2 and H-3 to the carboxy carbonyl C-1 along with COSY data revealed the presence of a nine-carbon tetraenoic acid unit from the C-1 carbonyl to C-9, with *J*-values indicating an all-*trans* configuration. Despite signal overlap, a 1-methyl-1-propenyl side-chain (C-20 to C-23) was recognized on the basis of a COSY correlation of H_3-22 (d, 6.7 Hz) with H-21 and HMBC correlations from H_3-22 and H_3-23 to olefinic carbons 20 and 21. One of these methyls (H_3-23) also showed a correlation to nonprotonated oxygen-bearing carbon C-19, showing the position of attachment of this methylpropenyl unit at C-19. H-9 of the tetraenoic side chain also showed HMBC correlations to C-19 as well as the other oxygenated, nonprotonated sp^3 carbon (C-10), placing these two side-chains on adjacent carbons (C-10 and C-19) and making a key connection between C-10 and C-19. Direct connection of C-9 to C-10 was confirmed by an HMBC correlation of H-8 to C-10. An additional correlation of H-9 with sp^3 aliphatic methine C-11 required linkage of C-10 and C-11. An extended spin-system comprising most of the rest of the molecule was evident from COSY and HMBC data (Figure 3), with the latter including key correlations from the remaining olefinic methyl H_3-24 to methylene C-15 and from olefinic H-17 to C-19 to establish the remaining linkages

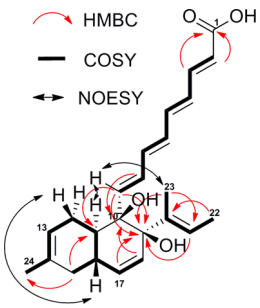

Figure 3. Key 2D NMR correlations used for structural characterization.

and complete the remainder of the decalin-type subunit in revised structure **1** (Figure 2).

Table 1 shows the NMR assignments for **1** with the new numbering according to the revised structure, the relative enrichments observed in ^{13}C NMR spectra of [1-^{13}C]-acetate-, [2-^{13}C]-acetate-, and [Me-^{13}C]-methionine-labeled campafungin A, and $^{1}J_{C-C}$ couplings observed in [1,2-$^{13}C_2$]-acetate-labeled campafungin A ^{13}C NMR spectra. Aside from the olefin geometry in the tetraenoic acid side-chain, the stereochemical features of **1** were difficult to ascertain with confidence due in part to the overlap of key signals, but collection of NOESY data in both $CDCl_3$ and DMSO-d_6 afforded correlations useful in assigning the relative configuration (Figures S14 and S15).The methylpropenyl side-chain could be assigned the *E*-geometry as shown on the basis of the upfield ^{13}C NMR shifts of both methyl groups (δ 13.8 and 14.0). NOESY correlations of H-9 with H-11 and H_3-23 and between H-11 and H_3-23 placed the nine-carbon side chain on the same face of the ring system as bridgehead hydrogen H-11 and the methylpropenyl substituent and required H-11 and the methylpropenyl group to be 1,3-diaxial (or pseudodiaxial). A NOESY correlation between H-16 and the pseudoaxial hydrogen at C-12 supported the *trans* ring fusion and completed the relative configuration as shown for structure **1**.

The revised structure for **1** was consistent with the NMR data acquired on the original sample. The C-10 (δ_H 4.18) and C-19 (δ_H 4.73) hydroxy protons were observed as sharp singlets, since the original data were acquired in DMSO-d_6. HMBC correlations from the 10-OH were observed to C-9, C-10, C-11, and C-19. HMBC correlations from the 19-OH were

https://dx.doi.org/10.1021/acs.jnatprod.0c00641
J. Nat. Prod. XXXX, XXX, XXX−XXX

Table 1. ^{1}H and ^{13}C NMR Assignments for Campafungin A (1; ^{1}H 500 MHz, ^{13}C 125 MHz, $CDCl_3$), Relative Enrichments Observed in ^{13}C NMR Spectra of [1-^{13}C]-Acetate-, [2-^{13}C]-Acetate-, and [Me-^{13}C]-Methionine-Labeled 1, and $^{1}J_{C-C}$ Coupling Observed in ^{13}C NMR Spectrum of [1,2-$^{13}C_2$]-Acetate-Labeled 1

no.	δ_C, mult	δ_H, mult (J in Hz)	HMBC (H→C)	relative enrichment [1-^{13}C] acetate[a]	relative enrichment [2-^{13}C] acetate[a]	relative enrichment [Me-^{13}C] methionine[b]	$^{1}J_{CC}$, Hz (J partner)
1	172.1, C			2.4	0.0	0.0	74.1 (2)
2	119.5, CH	5.86, d (15)	1, 3, 4	−0.2	1.9	−0.1	74.1 (1)
3	146.7, CH	7.39, dd (11, 15)	1, 2 4, 5	1.9	−0.1	0.0	56.6 (4)
4	129.6, CH	6.35, dd (11, 15)	2, 3, 6	−0.2	1.9	0.0	56.6 (3)
5	141.9, CH	6.62, dd (11, 15)	3, 6, 7	2.0	−0.1	−0.1	57.3 (6)
6	131.2, CH	6.32, dd (11, 14)	5, 7, 8	−0.1	1.9	0.0	57.3 (5)
7	137.1, CH	6.44, dd (9.9, 14)	5, 6, 8	2.0	−0.1	0.0	56.8 (8)
8	129.4, CH	6.47, dd (9.9, 14)	6, 7, 9, 10	−0.2	1.8	0.0	56.8 (7)
9	139.5, CH	5.56, d (14)	8, 9, 10, 11, 19	2.0	−0.1	−0.1	50.1 (10)
10	77.4, C	2.66, s (10-OH)		−0.1	1.4	0.0	50.1 (9)
11	39.2, CH	1.87, m	9, 12, 15, 19	1.7	−0.1	−0.1	35.6 (12)
12	26.5, CH_2	a: 1.86, m	11, 13, 14, 16	−0.2	1.7	−0.2	35.6 (11)
		b: 1.76, m	13, 14				
13	121.6, CH	5.37, d (3.6)	11, 15, 24	1.9	−0.1	−0.2	72.3 (14)
14	133.3, C			−0.1	1.7	−0.2	72.3 (13)
15	36.7, CH_2	a: 2.12, dd (4.5, 16)	11, 13, 14, 16, 24	1.8	−0.1	−0.2	34.4 (16)
		b: 1.85, m	13, 14, 16				
16	33.6, CH	2.27, m	11, 15, 17	−0.2	1.4	−0.2	34.4 (15)
17	131.1, CH	5.76, dd (1.7, 10)	11, 15, 16, 19	1.9	−0.1	−0.1	[c]
18	130.7, CH	5.29, dd (2.5, 10)	10, 16	−0.2	1.9	−0.1	[c]
19	80.3, C	3.48, s (19-OH)		1.7	−0.1	−0.1	48.3 (20)
20	136.9, C			0.1	1.9	−0.1	48.3 (19)
21	125.9, CH	5.55, m	19, 20, 22	1.6	−0.1	−0.1	43.8 (22)
22	14.0, CH_3	1.65, d (6.7)	20, 21	−0.1	2.0	−0.2	43.8 (21)
23	13.8, CH_3	1.64, s	10, 19, 21	0.0	0.0	24.4	
24	23.3, CH_3	1.67, s	13, 14, 15	0.0	0.0	24.1	

[a]Relative enrichments were normalized to peak intensity of the C-24 signal. [b]Relative enrichments were normalized to peak intensity of the C-1 signal. [c]Not observed due to overlap.

observed to C-10, C18, C-19, and C-20. The newly proposed structure for **1** places it in a class of decalin-containing polyketides produced by fungi that includes the monacolins, fusarielins, tanzawaic acids, cladobotric acids, anthracobic acids, and decalpenic acid.[17] Notably, the relative configuration assigned for **1** matches that reported for several of these compounds that share similar features with F2928-1 and -2, cladobotric acids, decalpenic acid, and anthracobic acids also containing carboxy-terminated chains with extended conjugation at the same position.

Efforts to assign absolute configuration by obtaining a crystal of **1** or a derivative or to apply ECD methods to this issue were unsuccessful. However, a few other members of this class with matching relative stereochemical features have had absolute configuration assigned, including fusarielin A[18] and cladobotric acid A.[19] These compounds were found to have absolute configurations analogous to each other, and we propose that campafungin A and the analogues discussed below are members of the same stereochemical family.

Structural Characterization of Campafungin A Analogues. Compound **2** (campafungin B) was recognized as an isomer of campafungin A on the basis of HRESIMS data. ^{1}H, ^{13}C, and 2D NMR data for **2** (Figures S16−S21; Table 2) were very similar to those of **1**; however, some differences could be noted. One clear difference was that C-10 lacked an OH group, as it appeared as a methine at δ_C 52.6 bearing a hydrogen at δ_H 2.08 that was coupled to H-9 of the tetraenoic acid side-chain. In addition, the signals for olefinic hydrogens H-17 and H-18 were absent and replaced by an AB pattern at δ_H 3.20/3.21 (J = 3.7 Hz), which correlated, by HSQC, with ^{13}C NMR signals at δc 59.7 and 60.4, indicating the presence of a C17−C18 epoxide in place of the olefin unit found in **1**. The NMR data were consistent with maintenance of the same relative configuration at stereocenters shared with **1**. Compound **2** was the only analogue encountered that lacked an OH substituent at C-10, but the signal for H-10 was well resolved and showed a large *trans*-diaxial J-value with H-11, as expected for the configuration shown, which retains the pseudoequatorial orientation of the tetraene-containing side-chain. The newly present epoxide hydrogens did not show stereochemically useful NOE correlations, but the ^{1}H and ^{13}C NMR chemical shifts, the J-value observed between the epoxide

https://dx.doi.org/10.1021/acs.jnatprod.0c00641
J. Nat. Prod. XXXX, XXX, XXX−XXX

Table 2. NMR Spectroscopic Data for 2−4 (^{1}H 500 MHz, ^{13}C 125 MHz, $CDCl_3$)

	2			3			4		
no.	δ_C	δ_H, mult. (J in Hz)	HMBC H→C	δ_C	δ_H, mult. (J in Hz)	HMBC H→C	δ_C	δ_H, mult. (J in Hz)	HMBC H→C
1	170.3			170.0			175.6		
2	119.1	5.87, d (15)	1, 4	120.0	5.87, d (15)	1, 4	119.5	5.93, d (15)	1, 4
3	146.7	7.38, dd (11, 15)	1, 5	141.1	7.85, dd (11, 15)	1, 2, 4, 5	146.6	7.50, dd (11, 15)	1, 4, 5
4	129.5	6.36, dd (11, 15)	2, 3, 5, 6	126.1	6.15, t (11)	2, 6	130.2	6.37, dd (11, 14)	3, 6
5	141.8	6.59, dd (11, 15)	3, 7	138.1	6.39, t (11)	3, 7	136.9	7.17, dd (11, 14)	3, 7
6	130.6	6.25, dd (11, 15)	4, 5, 7, 8	126.7	6.80, dd (11, 14)	4, 5, 8	127.8	6.07, t (11)	5, 7, 8
7	137.2	6.39, dd (11, 15)	5, 6, 8, 9	137.0	6.42, dd (11, 14)	5, 9	133.4	6.24, t (11)	5, 9
8	132.9	6.18, dd (11, 15)	6, 7, 10	129.5	6.52, dd (11, 15)	6, 10	124.8	6.94, dd (11, 15)	6, 7, 10
9	136.1	5.38, dd (11, 15)	7, 10, 11	139.5	5.54, m	8, 10, 11	139.6	5.54, d (15)	8,10,11
10	52.6	2.08, t (11)	8,9,11,19	76.9			77.6		
11	36.2	1.48, m		39.3	1.89, m	15, 16, 19	39.2	1.92, m	15, 16, 19
12	31.4	a: 1.79, m		26.5	a: 1.86, m		26.5	a: 1.88, m	
		b: 1.48, m	13, 14		b: 1.77, m	13, 14		b: 1.78, m	13, 14
13	121.6	5.34, br s	10, 11, 15, 24	121.6	5.37, d (4.0)	11, 24	121.6	5.40, d (4.0)	11, 24
14	133.6			133.3			133.2		
15	35.6	a: 2.14, dd (4.7, 14)	13, 14, 16, 24	36.7	a: 2.12, dd (4.5, 16)b: 1.85, m	11, 13, 16, 17, 24 13, 14, 24	36.9	a: 2.14, dd (4.3, 15)	11, 13, 17, 24 13, 14, 24
		b: 1.97, br t (14)	24					b: 1.86, m	
16	36.9	1.80, m	11, 12, 18	33.6	2.28, m	15, 18	33.6	2.32, m	
17	59.7	3.20, d (3.7)	15, 16	131.0	5.76, dd (1.3, 10)	11, 15, 16, 19	131.4	5.79, dd (1.5, 10)	11, 15, 16, 19
18	60.4	3.21, d (3.7)	10, 19	130.8	5.29, dd (2.3, 10)	10, 16	130.5	5.31, dd (2.5, 10)	10, 16
19	77.3			80.2			80.4		
20	136.6			136.9			137.0		
21	123.0	5.45, dq (6.3, 1.1)	19, 22, 23	125.8	5.55, m	19, 20, 23	125.9	5.58, m	19, 20, 23
22	14.4	1.69, d (6.3)	20	14.0	1.63, m	20, 21	14.0	1.63, d (5.6)	20, 21
23	13.6	1.68, d (1.1)	19	13.8	1.65, m	19	13.8	1.67, m	19
24	23.2	1.70 s	13	23.3	1.67, m	13, 14, 15	23.3	1.69, m	13, 14, 15

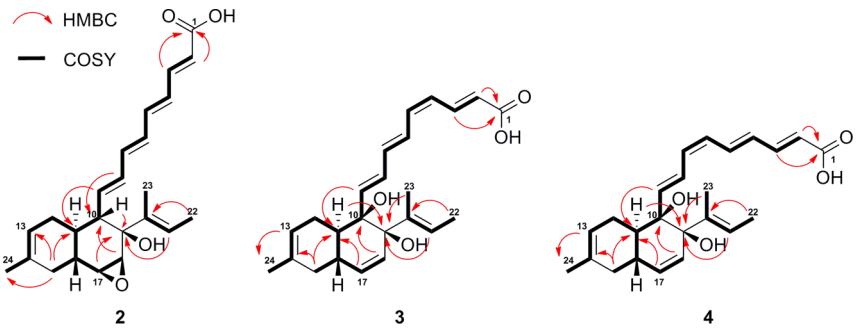

Figure 4. Key COSY (bold line) and selected HMBC (red arrows) correlations for 2−4.

hydrogens, and the *ca.* 0 Hz coupling between H-17 and bridgehead H-16 were nearly identical to the data for other decalin-containing compounds having an epoxide at this location on the same face as H-16.[20,21] Efforts to obtain a crystal for possible X-ray analysis in an effort to confirm this assignment were unsuccessful. All other features matched well with those of **1**. Thus, the structure of **2** was assigned as shown in Figure 4.

Campafungins C (**3**) and D (**4**) also proved to be isomers of **1**, with the molecular formula $C_{24}H_{30}O_4$ on the basis of HRESIMS analysis. Both compounds afforded 1D and 2D NMR data that were even more similar to those of **1** (Figures S22−S33; Table 2). Inspection of the ^{1}H NMR data revealed that the only significant difference in each case was in the olefin geometry at positions along the tetraenoic side-chain. The data for **3** indicated a *cis* relationship between H-4 and H-5, due to upfield chemical shifts of both resonances and their

https://dx.doi.org/10.1021/acs.jnatprod.0c00641
J. Nat. Prod. XXXX, XXX, XXX−XXX

smaller coupling value (J = 11 Hz). Similarly, the data for **4** showed upfield shifts and a smaller coupling value for H-6 and H-7 indicating a *cis* relationship between H-6 and H-7. In each case, all of the other side-chain olefins retained the *trans* geometry. The structures were otherwise identical to that of **1**, as supported by analysis of 2D NMR data.

A proposed biosynthetic pathway for campafungin A and its analogues is summarized briefly in Figure 5 based on common

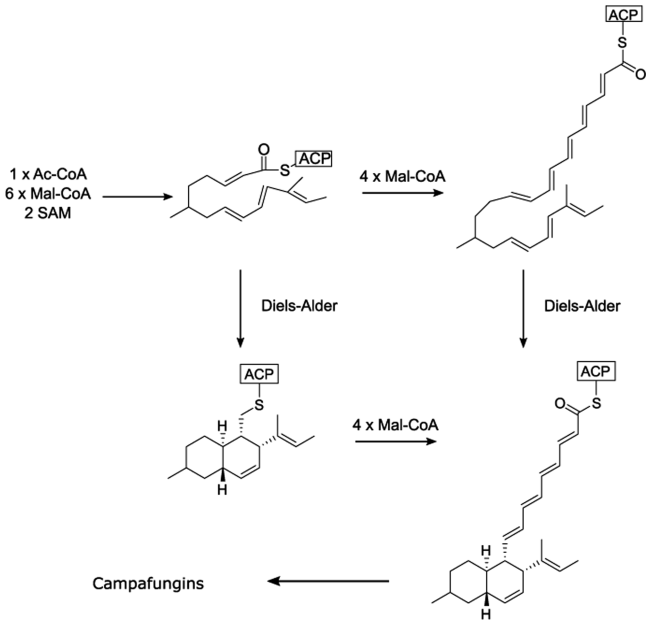

Figure 5. Proposed biosynthetic pathway to campafungins.

biosynthetic pathways described for other classes of decalin-containing polyketides, including equisetin,[22] fusarielin,[23] and lovastatin,[24] and is fully consistent with the isotope labeling results.

Antimicrobial Activity of Campafungins. The antifungal activity of *P. enteroleucus* crude extracts against *C. albicans* was confirmed by zone-of-inhibition assays. Similar assays also showed smaller zones of activity against *Staphylococcus aureus* and *Cryptococcus neoformans* (Figure S2). Purified compounds **1**–**4** were assayed against strains of *S. aureus*, *C. tropicalis*, *C. glabrata*, *C. albicans*, *C. neoformans*, and *A. fumigatus* in liquid serial dilution assays (Table 3). All four campafungins inhibited growth of most of the tested pathogens to some degree. However, with the exception of *C. neoformans*, none of the compounds showed any strong activity in liquid assays. In contrast to zone-of-inhibition assays, where *C. albicans* appeared more sensitive based on zone diameter, *C. neoformans* H99 was the most sensitive to the tested compounds in liquid assays, with MICs in the 4–8 μg mL^{-1} range.

To assess the antifungal activity of campafungin A against fungal strains of high medical relevance, the MIC was determined for *C. albicans* SC3514 and *A. fumigatus* AF293. While the MIC of campafungin A for *C. neoformans* H99 was consistently in the range of 8–10 μg mL^{-1}, the MIC at 48 h for *A. fumigatus* was higher, at 38 μg mL^{-1}; however, hyphal extension was notably inhibited at concentrations of 10 μg mL^{-1}. Also, *C. albicans* hyphal formation was transiently inhibited by 10 μg mL^{-1} campafungin A for 24–48 h, although there was an eventual recovery from the growth inhibition with longer incubation times, suggesting a fungistatic effect in this strain.

Table 3. Minimum Inhibitory Concentrations (MICs) of Campafungins A–D (1–4)

	compound (MIC; μg mL^{-1})				
organism	**1**	**2**	**3**	**4**	control[a]
Staphylococcus aureus ATCC 43300	64	32	32	32	0.05
Candida albicans ATCC 10231	128	128	128	>128	0.36
Candida tropicalis ATCC 750	64	64	64	64	0.36
Candida glabrata ATCC 2001	>128	>128	>128	>128	0.18
Cryptococcus neoformans H99	8	4	4	8	0.36
Aspergillus fumigatus FSGC A1240	64	64	64	64	0.74

[a]Chlortetracycline + streptomycin was used as control for *S. aureus*. Amphotericin B was used as control for other strains.

Campafungin Mode of Action Studies in *C. neoformans*. To further assess the antifungal mechanism of action for campafungin A (**1**), a library of 3880 *C. neoformans*-targeted mutant strains[25] was screened for increased drug resistance compared to wild-type, as marked by vigorous growth on medium containing 38 μg mL^{-1} campafungin A. Of 92 campafungin-resistant mutants (Table S1), 36 had mutations in genes encoding proteins of unknown function. Other strains included seven mutants in processes related to lipid metabolism or membrane integrity, six with mutations in carbon metabolism or polysaccharide capsule production, six in non-efflux transporter proteins, two in cell wall chitin/chitosan formation, and seven in processes involved in cellular regulation. Mutations in two efflux pumps were also associated with lower MICs, likely related to increased intracellular accumulation of campafungin A.

Interestingly, mutants in the *C. neoformans* PKA/cAMP pathway displayed MICs identical to that of the wild-type. These strains included those with mutations in genes encoding the G-alpha proteins Gpa1; adenylyl cyclase Cac1; protein kinase A catalytic and regulatory subunits Pka1 and Pkr1, respectively; and phosphodiesterase Pde1.[26] Additionally, subinhibitory concentrations of campafungin A did not affect the expression of two virulence-associated phenotypes associated with cAMP signaling in this fungus: encapsulation and melanin production (data not shown). Lastly, complete genetic blocking of cAMP signaling does not significantly affect fitness of *C. neoformans in vitro*,[27] suggesting that additional mechanisms of cellular inhibition must explain the antifungal activity of campafungin A in this species.

Given the relative resistance of two *C. neoformans* strains with predicted mutations in efflux-related processes, we tested the activity of campafungin A against a *Schizosaccharomyces pombe* strain with multiple mutations impairing drug efflux mechanisms. This strain has been used by other investigators to assess the role of efflux-mediated drug inactivation for other antifungal compounds.[28,29] The isogenic wild-type strain displayed an MIC for campafungin A of 10 μg/mL^{-1}. In contrast, the *S. pombe* efflux mutant strain was more susceptible, with an MIC of 2 μg/mL^{-1}, suggesting that compound efflux affects campafungin A activity across fungal species.

https://dx.doi.org/10.1021/acs.jnatprod.0c00641
J. Nat. Prod. XXXX, XXX, XXX−XXX

In summary, our studies of campafungin A (**1**) have clarified its structure as a new, but more typical, decalin-type polyketide when compared to the originally proposed structure. The producing strain also yielded several minor analogues identified here as campafungins B, C, and D (**2**–**4**). We have also demonstrated that the antifungal activity and hyphal inhibition effects of campafungins extend to other fungal species beyond the original report in *C. albicans*. Liquid dilution assays indicated that *C. neoformans* was the most sensitive of the species tested. We were unsuccessful in identifying a mode-of-action in *C. neoformans*. Nevertheless, the repression of hyphal extension in multiple species, and especially in *C. albicans* as reported previously, points to campafungin A as a potentially useful compound for understanding mechanisms of yeast-to-hyphae transition and their role in fungal virulence.

EXPERIMENTAL SECTION

General Experimental Procedures. Extracts were fractionated on a Grace Reveleris X2 flash chromatography system with UV and ELSD detectors. HPLC-DAD-MS analysis employed an Agilent 1260 LC coupled to an Agilent 6120 single quadrupole MS with 0.1% aqueous formic acid (A), MeOH (B), and 0.1% formic acid in acetonitrile (C) as mobile phases. Chromatographic profiles were monitored by scanning from 190 to 400 nm with acquisition set at 330 nm and by positive and negative ESIMS at m/z 160−1500. NMR data were collected at 298 K on a Bruker 500 MHz NMR instrument equipped with a 5 mm triple resonance cryoprobe, with $CDCl_3$ as solvent and tetramethylsilane used as internal standard (TMS δ_H 0).

Fungal Strain and Fermentation. Fungal strain F-146,176 was isolated from leaf litter of *Fraxinus angustifolia*, Los Molinos, Virgen de Espino, Madrid, Spain (Figure S1, Supporting Information). This strain originated from the former Centro de Investigación de España, Merck Sharp & Dohme de España natural products library, and is maintained as frozen mycelium in 10% glycerol at −80 °C at the Natural Products Discovery Institute, the Baruch S. Blumberg Institute, Doylestown, Pennsylvania, USA.

Strain F-146,176 was grown on five media in 12 mL fermentations to confirm the original antifungal activity and the presence of campafungin(s). For the seed culture, six agar discs from 2-week-old YM agar (malt extract 10 g, yeast extract 2 g, agar 20 g, 1000 mL of deionized H_2O) cultures were inoculated into SMY (maltose 40 g, neopeptone 10 g, yeast extract 10 g, 1000 mL of deionized H_2O) with 0.4% agar in 50 mL aliquots in a 250 mL flask. Seed cultures were grown at 24 °C, 220 rpm for 4 d. For the production cultures, 1 mL aliquots of the seed growth were transferred to 50 mL glass vials with 12 mL of Wheat 1 medium (5 g whole wheat seeds, 8.5 mL of base liquid consisting of yeast extract 2 g, sodium tartrate 10 g, KH_2PO_4 1 g, $MgSO_4{\cdot}7H_2O$ 1 g, $FeSO_4{\cdot}7H_2O$ 0.050 g, 1000 mL of deionized H_2O), CYS80 (sucrose 80 g, yellow cornmeal 50 g, yeast extract 1 g in 1000 mL of deionized H_2O), MMK2 (mannitol 40 g, yeast extact 5 g, Murashige & Skoog salts [Sigma-Aldrich M-5524] 4.3 g, in 1000 mL of deionized H_2O), MPP (maltose 25 g, glucose 10 g, dried baker's yeast 5 g, Pharmamedia [Archer Daniels Midland] 10 g, in 1000 mL of deionized H_2O), and GS (glucose 25 g, corn starch 10 g, blackstrap molasses (Brer Rabbit) 5 g, casein hydrolysate 4 g, meat peptone 1 g, 1000 mL of deionized H_2O), respectively. Cultures on the Wheat 1 and CYS80 media were incubated statically with vials slanted at a 45° angle; the other media were agitated at 220 rpm. For quantitative measurements of titers, five replicates of each fermentation were grown at 24 °C for 12 d.

For large-scale cultivation, five agar plugs of a one-week culture of strain F-146,176 grown in YM agar were transferred to a 500 mL flask containing 100 mL of SMY medium. The seed medium was grown for 7 days at 23 °C and 180 rpm; then 5 mL of growth was transferred to each of six 1.0 L Roux bottles each containing 125 mL of Wheat 1 medium and kept static at 23 °C for 21 days.

To obtain labeled campafungin A, 100 mg/mL solutions of [1-^{13}C], [2-^{13}C], and [1,2-$^{13}C_2$] acetate were prepared in deionized water and filter sterilized with 0.22 μM nylon membranes. A solution of [Me-^{13}C]-L-methionine was prepared with a final concentration of 33.3 mg/mL. The seed stage was grown in GS medium. For each labeling experiment, five 500 mL flasks containing 100 mL of GS medium were inoculated with 7 mL of seed culture. The production culture was grown under the same conditions, spiked on day 4, 8, and 11 with the labeled solutions individually (0.33 mL of acetate or 1.00 mL of methionine solution per flask each time), and extracted after 14 days of growth. Each flask received 0.1 g/L of labeled precursor overall.

DNA Sequencing and Characterization of Fungal Strain F-146,176. Methods for total genomic DNA extraction, PCR amplification, primers, and sequencing of the rDNA region containing the partial 28S sequence including the D1, D2, and internal transcribed spacer regions have been described previously.[8,9] The concatenated sequences of large subunit (LSU) 28S (GenBank MN910294) and intertranscribed spacer (ITS) rDNA (GenBank MN910295) were compared with a previous alignment of fungi of various genera of the Leptosphaeriaceae.[15] The resulting alignment was used to generate a maximum likelihood phylogenetic analysis implemented in MEGA 7.[30]

Purification of Campafungins. Campafungins were extracted by the addition of methyl ethyl ketone (MEK) to each flask (350 mL for each Roux bottle with Wheat 1 medium; 100 mL for each flask of GS medium) and then agitated on an orbital shaker for 2 h. The dark red extract was vacuum filtered, and the organic layers were combined and separated, reduced to approximately 50 mL, adsorbed onto silica gel, and finally evaporated to dryness. The silica saturated with the crude extract was loaded on top of a C_{18} vacuum liquid chromatography column and eluted with MeOH−H_2O (8:2 v/v) to obtain a golden eluate that was evaporated to dryness, yielding 1.42 g. The sample was submitted to flash chromatography (Reveleris C_{18} RP 40 g cartridge, 70% MeOH for 3 min, then 70−90% MeOH for 2 min and held for 7 min at a flow rate of 30 mL min^{-1}). Fractions containing campafungin were monitored by UV at 330 nm, collected, pooled, and dried, weighing 0.93 g. The campafungin-rich fraction (0.5 g) was dissolved in MeOH and further purified by semi-preparative HPLC (Zorbax SB-C_{18} column 9.4 × 250 mm, 5 μm, 30 °C; 15% A/85% B for 3 min, 85−90% B for 5 min, 90−100% B for 8 min, held for 2 min, at 4.0 mL/min), yielding 127 mg of campafungin A (**1**) and 7.2 mg of campafungin B (**2**). Campafungins C and D eluted as a mixture and were further separated using semipreparative HPLC (Zorbax SB-C_{18} column 9.4 × 250 mm, 5 μm, 30 °C; 40% A/60% C initial, up to 70% C over 20 min at 4.0 mL/min), yielding 3.1 mg of campafungin C (**3**) and 2.3 mg of campafungin D (**4**). Flash chromatography fractions were checked by HPLC-DAD-MS (Ace Equivalence C_{18}, 4.6 × 150 mm, 5 μm, 30 °C; 30% A/70% B for 3 min, 70−100% B in 10 min, held for 4 min, at 1.0 mL/min), and purity of peaks was checked using another method (Ace Equivalence C_{18}, 4.6 × 150 mm, 5 μm, 30 °C; 40% A/60% C initial, up to 70% C over 20 min at 1.0 mL/min).

*Campafungin A (**1**):* light yellow powder, $[\alpha]_D$ −48 (c 0.027, MeOH); UV (MeOH) λ_{max} (log ε) 205 (4.0), 322 (4.2); NMR data ($CDCl_3$), Table 1; HRESIMS m/z 381.2071 $[M - H]^-$ (calcd for $[C_{24}H_{30}O_4 - H]$, m/z 381.2066).

*Campafungin B (**2**):* light yellow powder, $[\alpha]_D$ −104 (c 0.007, MeOH); UV (MeOH) λ_{max} (log ε) 203 (4.6), 322 (4.4); NMR data ($CDCl_3$), Table 2; HRESIMS m/z 381.2073 $[M - H]^-$ (calcd for $[C_{24}H_{30}O_4 - H]$, m/z 381.2066).

*Campafungin C (**3**):* light yellow powder, $[\alpha]_D$ −65 (c 0.127, MeOH); UV (MeOH) λ_{max} (log ε) 203 (4.2), 234 (4.2), 322 (4.4); NMR data ($CDCl_3$), Table 2; HRESIMS m/z 381.2076 $[M - H]^-$ (calcd for $[C_{24}H_{30}O_4 - H]$, m/z 381.2066).

*Campafungin D (**4**):* light yellow powder, $[\alpha]_D$ −51 (c 0.073, MeOH); UV (MeOH) λ_{max} (log ε) 204 (4.2), 322 (4.3); NMR data ($CDCl_3$), Table 2; HRESIMS m/z 381.2082 $[M - H]^-$ (calcd for $[C_{24}H_{30}O_4 - H]$, m/z 381.2066).

https://dx.doi.org/10.1021/acs.jnatprod.0c00641
J. Nat. Prod. XXXX, XXX, XXX−XXX

Screening for Growth Inhibition of *C. albicans* and *C. neoformans* and Selection of Extracts for the CaFT. The antifungal activity produced by strain F-146,176 was initially detected in agar zone of inhibition assays with extracts from 12 mL fermentations as described previously.[3] To confirm that strain F-146,176 still produces campafungins, extracts from Wheat 1, CYS80, MMK2, MPP, and GS media were tested for antifungal activity. Each fermentation was extracted by the addition of an equal volume of MEK followed by shaking for 2 h. The MEK layer was evaporated under vacuum. Residues were dissolved in DMSO at 10× the original culture volume, and 20 μL of each DMSO extract was applied to a 4 mm well aspirated from a plate of YM agar (malt extract 10 g, yeast extract 2 g, agar 20 g, in 1000 mL of deionized H_2O) seeded with an overnight culture of *S. aureus* ATCC 43300, *C. albicans* ATCC 10231, or *C. neoformans* H99. Plates were incubated at 25 °C and examined after 24−48 h, and zones of inhibition were photographed.

Antimicrobial Activities. To quantify the inhibitory concentrations of campafungins for various strains of fungal and bacterial pathogens, MICs were measured using species-specific modifications to standard CLSI testing methods.[31] For each fungus, cells or spores (in the case of *A. fumigatus*) were sequentially diluted in PBS and RPMI-1640 buffered with MOPS (Sigma-Aldrich). The final cell suspension was incubated with serial dilutions of campafungins at a dose range of 1−355 μM. Growth was assessed by adding 10% resazurin (alamarBlue, Bio-Rad) and incubation for 24 h (*S. aureus*), 48 h (*Candida* spp. and *A. fumigatus*), or 72 h (*C. neoformans* and *S. pombe*). Viability was measured by fluorescence detected after the reduction of resazurin to resorufin as directed by the manufacturer (Bio-Rad). Additionally, growth dynamics and cellular morphogenesis were assessed microscopically every 24 h for all experimental samples.

Strains tested included *Staphylococcocus aureus* ATCC 43300, *Candida tropicalis* ATCC 750, *Candida glabrata* ATCC 2001, *Candida albicans* ATCC10231, *Aspergillus fumigatus* FSGC A1240, and *Cryptococcus neoformans* H99. The following pathogenic fungal strains were also tested: *C. albicans* SC3514 and *A. fumigatus* AF293. Additionally, the *Schizosaccharomyces pombe* strain SAK1 and the isogenic efflux mutant MJ-1682[28] were also tested in this assay, using YPD medium (Becton Dickinson), to address known auxotrophies. Other strains tested included the *C. neoformans* cAMP pathway mutants (H99 strain background): AAC1 (*gpa1*Δmutant);[27] RPC3 (*cac1*Δmutant);[32] CDC1 (*pka1*Δmutant);[33] CDC7 (*pkr1*Δmutant);[33] and JKH63 (*pde1*Δmutant).[34]

Assessment of cAMP-Related Phenotypes. *C. neoformans* capsule formation in the presence and absence of campafungin was assessed using standard India ink counterstaining after incubation for 72 h in CO_2-independent medium (Gibco), a capsule-inducing condition. *C. neoformans* melanin production was assessed by pigment changes at 72 h of incubation in minimal medium containing L-DOPA as previously described.[27]

***C. neoformans* Mutant Screen.** To identify strains with altered susceptibility to campafungin A, a large mutant collection[35] (available as the Madhani 2015/2016 plates, Fungal Genetics Stock Center) was tested for relative resistance to the compound by assessing for viability after exposure to 100 μM campafungin A in yeast nitrogen base medium (YNB; Becton Dickinson), with 1.8% (w/v) glucose for 48 h. To aid in visual high-input screening, 0.002% resazurin was added to YNB.[36] Viability was visually assessed by the color change produced by the reduction of resazurin (blue) to resorufin (pink) then to hydroresorufin (colorless). In addition, the campafungin-treated mutant strains were plated onto YPD to confirm resistance. Individual resistant strains were then retested in secondary screens for confirmation of relative resistance as compared to wild-type strain H99.

■ ASSOCIATED CONTENT

Supporting Information

The Supporting Information is available free of charge at https://pubs.acs.org/doi/10.1021/acs.jnatprod.0c00641.

^{1}H NMR, ^{13}C NMR, and 2D NMR spectra and MS data for compounds **1**−**4** (PDF)

■ AUTHOR INFORMATION

Corresponding Author

Gerald F. Bills − *Texas Therapeutics Institute, The Brown Foundation Institute of Molecular Medicine, University of Texas Health Science Center at Houston, Houston, Texas 77054, United States;* orcid.org/0000-0003-2352-8417; Phone: 01-713-486-2344; Email: billsge@vt.edu, Gerald.F.Bills@uth.tmc.edu

Authors

Bruno Perlatti − *Texas Therapeutics Institute, The Brown Foundation Institute of Molecular Medicine, University of Texas Health Science Center at Houston, Houston, Texas 77054, United States*

Guy Harris − *Guy Harris Consulting, Belington, West Virginia 26250, United States*

Connie B. Nichols − *Departments of Medicine and Molecular Genetics & Microbiology, Duke University Medical Center, Durham, North Carolina 27710, United States*

Dulamini I. Ekanayake − *Department of Chemistry, University of Iowa, Iowa City, Iowa 52242, United States*

J. Andrew Alspaugh − *Departments of Medicine and Molecular Genetics & Microbiology, Duke University Medical Center, Durham, North Carolina 27710, United States*

James B. Gloer − *Department of Chemistry, University of Iowa, Iowa City, Iowa 52242, United States;* orcid.org/0000-0002-9261-7571

Complete contact information is available at: https://pubs.acs.org/10.1021/acs.jnatprod.0c00641

Author Contributions

The manuscript was written through contributions of all authors. All authors have given approval to the final version of the manuscript.

Notes

The authors declare no competing financial interest.

■ ACKNOWLEDGMENTS

G.H. and G.F.B. acknowledge the work of their former colleagues from Merck Research Laboratories and Merck Sharp & Dohme de España, S.A., who made the initial discovery of campafungin A. We thank the Natural Products Discovery Institute of the Baruch S. Blumberg Institute for providing the campafungin-producing strain. We would also like to acknowledge funding from NIH R01GM121458 and the Madhani laboratory at UCSF, funded by R01AI100272, for the publicly available *C. neoformans* deletion mutant collection.

■ REFERENCES

(1) Xu, D.; Jiang, B.; Ketela, T.; Lemieux, S.; Veillette, K.; Martel, N.; Davison, J.; Sillaots, S.; Trosok, S.; Bachewich, C.; Bussey, H.; Youngman, P.; Roemer, T. *PLoS Pathog.* **2007**, *3*, e92.

(2) Xu, D.; Sillaots, S.; Davison, J.; Hu, W.; Jiang, B.; Kauffman, S.; Martel, N.; Ocampo, P.; Oh, C.; Trosok, S.; Veillette, K.; Wang, H.; Yang, M.; Zhang, L.; Becker, J.; Martin, C. E.; Roemer, T. *J. Biol. Chem.* **2009**, *284*, 19754−19764.

(3) Roemer, T.; Xu, D.; Singh, S. B.; Parish, C. A.; Harris, G.; Wang, H.; Davies, J. E.; Bills, G. F. *Chem. Biol.* **2011**, *18*, 148−164.

(4) Jiang, B.; Xu, D.; Allocco, J.; Parish, C.; Davison, J.; Veillette, K.; Sillaots, S.; Hu, W.; Rodriguez-Suarez, R.; Trosok, S.; Zhang, L.; Li,

Y.; Rahkhoodaee, F.; Ransom, T.; Martel, N.; Wang, H.; Gauvin, D.; Wiltsie, J.; Wisniewski, D.; Salowe, S.; Kahn, J. N.; Hsu, M. J.; Giacobbe, R.; Abruzzo, G.; Flattery, A.; Gill, C.; Youngman, P.; Wilson, K.; Bills, G.; Platas, G.; Pelaez, F.; Diez, M. T.; Kauffman, S.; Becker, J.; Harris, G.; Liberator, P.; Roemer, T. *Chem. Biol.* **2008**, *15*, 363−374.
(5) Parish, C. A.; Smith, S. K.; Calati, K.; Zink, D.; Wilson, K.; Roemer, T.; Jiang, B.; Xu, D.; Bills, G.; Platas, G.; Peláez, F.; Díez, M. T.; Tsou, N.; McKeown, A. E.; Ball, R. G.; Powles, M. A.; Yeung, L.; Liberator, P.; Harris, G. *J. Am. Chem. Soc.* **2008**, *130*, 7060−7066.
(6) Mann, P. A.; McLellan, C. A.; Koseoglu, S.; Si, Q.; Kuzmin, E.; Flattery, A.; Harris, G.; Sher, X.; Murgolo, N.; Wang, H.; Devito, K.; de Pedro, N.; Genilloud, O.; Kahn, J. N.; Jiang, B.; Costanzo, M.; Boone, C.; Garlisi, C. G.; Lindquist, S.; Roemer, T. *ACS Infect. Dis.* **2015**, *1*, 59−72.
(7) Wilson, K. E.; Smith, S. K.; Kelly, R.; Masurekar, P.; Xu, D.; Parish, C. A.; Wang, H.; Zink, D. L.; Davies, J. E.; Roemer, T. *J. Nat. Prod.* **2014**, *77*, 1280−1286.
(8) Ondeyka, J.; Harris, G.; Zink, D.; Basilio, A.; Vicente, F.; Bills, G.; Platas, G.; Collado, J.; González, A.; Cruz, M. d. l.; Martin, J.; Kahn, J. N.; Galuska, S.; Giacobbe, R.; Abruzzo, G.; Hickey, E.; Liberator, P.; Jiang, B.; Xu, D.; Roemer, T.; Singh, S. B. *J. Nat. Prod.* **2009**, *72*, 136−141.
(9) Herath, K.; Harris, G.; Jayasuriya, H.; Zink, D.; Smith, S.; Vicente, F.; Bills, G.; Collado, J.; González, A.; Jiang, B.; Kahn, J. N.; Galuska, S.; Giacobbe, R.; Abruzzo, G.; Hickey, E.; Liberator, P.; Xu, D.; Roemer, T.; Singh, S. B. *Bioorg. Med. Chem.* **2009**, *17*, 1361−1369.
(10) Bahn, Y. S.; Sundstrom, P. *J. Bacteriol.* **2001**, *183*, 3211−3223.
(11) Kumamoto, C. A.; Vinces, M. D. *Cell. Microbiol.* **2005**, *7*, 1546−1554.
(12) Banerjee, M.; Thompson, D. S.; Lazzell, A.; Carlisle, P. L.; Pierce, C.; Monteagudo, C.; López-Ribot, J. L.; Kadosh, D. *Mol. Biol. Cell* **2008**, *19*, 1354−1365.
(13) O'Meara, T. R.; Veri, A. O.; Ketela, T.; Jiang, B.; Roemer, T.; Cowen, L. E. *Nat. Commun.* **2015**, *6*, 6741.
(14) Qiao, Y.-N.; Jin, X.-Y.; Zhou, J.-C.; Zhang, J.-Z.; Chang, W.-Q.; Li, Y.; Chen, W.; Ren, Z.-J.; Zhang, C.-Y.; Yuan, S.-Z.; Lou, H.-X. *J. Nat. Prod.* **2020**, *83*, 1766−1777.
(15) de Gruyter, J.; Woudenberg, J. H. C.; Aveskamp, M. M.; Verkley, G. J. M.; Groenewald, J. Z.; Crous, P. W. *Stud. Mycol.* **2013**, *75*, 1−36.
(16) Weissman, K. J., Chapter 1 Introduction to Polyketide Biosynthesis. In *Complex Enzymes in Microbial Natural Product Biosynthesis, Part B: Polyketides, Aminocoumarins and Carbohydrates*; Academic Press, 2009; pp 3−16.
(17) Li, G.; Kusari, S.; Spiteller, M. *Nat. Prod. Rep.* **2014**, *31*, 1175−1201.
(18) Kobayashi, H.; Sunaga, R.; Furihata, K.; Morisaki, N.; Iwasaki, S. *J. Antibiot.* **1995**, *48*, 42−52.
(19) Mitova, M. I.; Lang, G.; Blunt, J. W.; Cummings, N. J.; Cole, A. L.; Robinson, W. T.; Munro, M. H. *J. Org. Chem.* **2006**, *71*, 492−7.
(20) Shiono, Y. *Chem. Biodiversity* **2006**, *3*, 217−23.
(21) Kumagai, H.; Someno, T.; Dobashi, K.; Isshiki, K.; Ishizuka, M.; Ikeda, D. *J. Antibiot.* **2004**, *57*, 97−103.
(22) Sims, J. W.; Fillmore, J. P.; Warner, D. D.; Schmidt, E. W. *Chem. Commun.* **2005**, *2*, 186−188.
(23) Droce, A.; Saei, W.; Jørgensen, S. H.; Wimmer, R.; Giese, H.; Wollenberg, R. D.; Sondergaard, T. E.; Sørensen, J. L. *Molecules* **2016**, *21*, 1710.
(24) Sorensen, J. L.; Auclair, K.; Kennedy, J.; Richard Hutchinson, C.; Vederas, J. C. *Org. Biomol. Chem.* **2003**, *1*, 50−59.
(25) Liu, O. W.; Chun, C. D.; Chow, E. D.; Chen, C.; Madhani, H. D.; Noble, S. M. *Cell* **2008**, *135*, 174−188.
(26) Pukkila-Worley, R.; Alspaugh, J. A. *FEMS Yeast Res.* **2004**, *4*, 361−367.
(27) Alspaugh, J. A.; Perfect, J. R.; Heitman, J. *Genes Dev.* **1997**, *11*, 3206−3217.
(28) Kawashima, S. A.; Takemoto, A.; Nurse, P.; Kapoor, T. M. *Chem. Biol.* **2012**, *19*, 893−901.
(29) Aoi, Y.; Kawashima, S. A.; Simanis, V.; Yamamoto, M.; Sato, M. *Open Biol.* **2014**, *4*, 140063.
(30) Stecher, G.; Kumar, S.; Tamura, K. *Mol. Biol. Evol.* **2016**, *33*, 1870−1874.
(31) Alexander, B. D. *Reference method for broth dilution antifungal susceptibility testing of yeasts. Approved standard M27−A4*, 4th ed.; Clinical and Laboratory Standards Institute: Wayne, PA, 2017.
(32) Alspaugh, J. A.; Pukkila-Worley, R.; Harashima, T.; Cavallo, L. M.; Funnell, D.; Cox, G. M.; Perfect, J. R.; Kronstad, J. W.; Heitman, J. *Eukaryotic Cell* **2002**, *1*, 75−84.
(33) D'Souza, C. A.; Alspaugh, J. A.; Yue, C.; Harashima, T.; Cox, G. M.; Perfect, J. R.; Heitman, J. *Mol. Cell. Biol.* **2001**, *21*, 3179−3191.
(34) Hicks, J. K.; Bahn, Y.-S.; Heitman, J. *Eukaryotic Cell* **2005**, *4*, 1971−1981.
(35) Chun, C. D.; Madhani, H. D. *Methods Enzymol.* **2010**, *470*, 797−831.
(36) Monteiro, M. C.; de la Cruz, M.; Cantizani, J.; Moreno, C.; Tormo, J. R.; Mellado, E.; De Lucas, J. R.; Asensio, F.; Valiante, V.; Brakhage, A. A.; Latgé, J.-P.; Genilloud, O.; Vicente, F. *J. Biomol. Screening* **2012**, *17*, 542−549.

https://dx.doi.org/10.1021/acs.jnatprod.0c00641
J. Nat. Prod. XXXX, XXX, XXX−XXX